An ANN-Based Approach for Prediction of Sufficient Seismic Gap between Adjacent Buildings Prone to Earthquake-Induced Pounding

Seyed Mohammad Khatami [1], Hosein Naderpour [2], Seyed Mohammad Nazem Razavi [3], Rui Carneiro Barros [4], Barbara Sołtysik [5,*] and Robert Jankowski [5]

[1] Center of Semnan Municipality, University of Applied Science and Technology, Semnan 98 23, Iran; m61.khatami@gmail.com

[2] Faculty of Civil Engineering, Semnan University, Semnan 3513119111, Iran; naderpour@semnan.ac.ir

[3] Faculty of Civil Engineering, Isfahan University, Isfahan 031, Iran; smn.razavi@gmail.com

[4] Faculty of Engineering, University of Porto (FEUP), 351-22 Porto, Portugal; rcb@fe.up.pt

[5] Faculty of Civil and Environmental Engineering, Gdansk University of Technology, 80-233 Gdansk, Poland; jankowr@pg.edu.pl

* Correspondence: barbara.soltysik@pg.edu.pl

check for updates

Abstract: Earthquake-induced structural pounding may cause major damages to structures, and therefore it should be prevented. This study is focused on using an artificial neural network (ANN) method to determine the sufficient seismic gap in order to avoid collisions between two adjacent buildings during seismic excitations. Six lumped mass models of structures with a different number of stories (from one to six) have been considered in the study. The earthquake characteristics and the parameters of buildings have been defined as inputs in the ANN analysis. The required seismic gap preventing pounding has been firstly determined for specified structural arrangements and earthquake records. In order to validate the method for other structural parameters, the study has been further extended for buildings with different values of height, mass, and stiffness of each story. Finally, the parametric analysis has been conducted for various earthquakes scaled to different values of the peak ground acceleration (PGA). The results of the verification and validation analyses indicate that the determined seismic gaps are large enough to prevent structural collisions, and they are just appropriate for all different structural arrangements, seismic excitations, and structural parameters. The results of the parametric analysis show that the increase in the PGA of earthquake records leads to a substantial, nearly uniform, increase in the required seismic gap between structures. The above conclusions clearly indicate that the ANN method can be successfully used to determine the minimal distance between two adjacent buildings preventing their collisions during different seismic excitations.

Keywords: seismic gap; structural pounding; earthquakes; artificial neural network

1. Introduction

It is obviously seen that an insufficient seismic gap between adjacent structures may provide damages due to possible collisions between them during seismic excitations. The phenomenon, which is often called "earthquake-induced structural pounding", concerns mainly buildings and bridges [1–6]. It occurs when the gap between structures, or structural members, cannot cover their relative movements, and the relative lateral displacement exceeds the seismic gap [7–12]. Therefore, the estimation of a sufficient gap provides a safety zone between adjacent buildings, preventing structural damage often observed during previous earthquakes [13–15].

The majority of building codes suggest determining the minimum in-between gap size for providing enough space in order to prevent building collisions. For this purpose, the absolute sum method (*ABS*) and the sum of the squares of the modal response (*SRSS*) are often used (see [16,17], for example). The formulae are defined as

$$S = \delta_i + \delta_j \tag{1}$$

$$S = \sqrt{\delta_i^2 + \delta_j^2} \tag{2}$$

where S is the gap size between buildings, and δ_i and δ_j denote the peak lateral displacement of building i and j, respectively. Other codes consider the structural height to determine the sufficient seismic gap between buildings, e.g., the following formula is used [18]:

$$S = 0.05(h_i + h_j) \tag{3}$$

where h_i and h_j are the heights of buildings i and j, respectively. Some other examples of recommendations can be found in the codes of different countries:

- Canada: sum of individual peak lateral displacements of structures calculated by elastic analyses;
- Turkey: 3 cm for 6 m of height of the building, and 1 cm should be added for every 3 m of height;
- Australia: more than 1% of the height of the structure;
- Serbia: min. 3 cm and should be increased by 1 cm for every 3 m of the height of the building;
- Peru: $3 + 0.004 \cdot (h - 500)$ cm;
- India: R times the sum of the calculated peak lateral displacements of the structures;
- Egypt: 2 times the sum of the peak displacements of the structures or 0.004 times the height of the building.

On the other hand, various researchers have generally studied different methods to evaluate the seismic gap, which is usually less conservative than the critical gap determined by the codes. Some of them suggest that the structural period and also the damping coefficient must also be considered in order to calculate the seismic gap. Consequently, the critical distance can be reduced in such a case. For example, Jeng et al. [19] suggested the equation based on the *SRSS* formula, which is described as

$$S = \sqrt{\delta_i^2 + \delta_j^2 - 2\rho_{op}\delta_i\delta_j} \tag{4}$$

where ρ_{op} is the cross-correlation coefficient determined as [19]:

$$\rho_{op} = \frac{8\sqrt{\zeta_i\zeta_j}\left(\zeta_j + \zeta_i\frac{T_j}{T_i}\right)\left(\frac{T_j}{T_i}\right)^{\frac{3}{2}}}{\left(1 - \left(\frac{T_j}{T_i}\right)^2\right)^2 + 4\zeta_i\zeta_j\left(1 + \left(\frac{T_j}{T_i}\right)^2\right)\frac{T_j}{T_i} + 4\left(\zeta_i^2 + \zeta_j^2\right)\left(\frac{T_j}{T_i}\right)^2} \tag{5}$$

where T_i and T_j are the periods of the buildings and ζ_i and ζ_j denote the structural damping ratios (see also [20]). Recently, Naderpour et al. [21] proposed a new formula for the cross-correlation coefficient, ρ_{op}, as a parameter of Equation (4), based on a cyclic process by using both periods of the buildings, and investigated the accuracy of the formula for different situations and various models so as to confirm the formula. In the approach, ρ_{op} is defined in the more general form as [21]

$$\rho_{op} = \left|\frac{T_j}{T_i} - 10.5\left(T_j - T_i\right)\right| \tag{6}$$

Further studies focused on the aspects of the minimum seismic gap between structures preventing their pounding were also conducted. Der Kiureghian [22] suggested the equation to calculate the seismic gap based on the structural vibration periods and damping ratios of buildings. Penzien [23]

recommended using an effective structural period in the formula for the optimum gap size. The minimum seismic gap between adjacent non-linear structures was analyzed by Garcia [24]. Kasai et al. [25] used the inelastic vibration phase theory for seismic pounding mitigation. The accuracy of different criteria for a separation large enough to prevent collisions between nonlinear hysteretic structural systems was evaluated by Lopez-Garcia and Soong [26]. A number of other studies concerned also different methods to control relative displacements between adjacent structures, reducing the pounding hazard by the application of various types of dampers, links, etc. (see [27–31], for example). Moreover, Anajafi et al. [32] evaluated the adequacy of the seismic gap prescribed by diffident building design codes and load standards (see also [33–36]). They conducted nonlinear response history analyses on many buildings with different lateral force resisting systems. Anajafi et al. [32] illustrated that, in many cases, the seismic gap prescribed by building design codes is exceeded significantly, especially when soil–structure interaction effects are taken into account.

The aim of the present paper is to show the results of the investigation focused on using an artificial neural network (ANN) method to conduct the evaluation of the optimum gap size between adjacent buildings, so as to prevent their collisions during seismic excitations. In the study, two structures with a different number of stories have been subjected to different earthquake records. To predict the appropriate distance between structures, the earthquake characteristics and the parameters of structures have been defined as inputs in the ANN model.

2. Materials and Methods

There are a number of different methods which can be used to predict different types of phenomena, including decision trees and risk analysis (see [37]), statistics and random algorithms (e.g., [38,39]), or artificial intelligence and machine learning (e.g., [40]). For the purposes of the present work, the ANN has been used so as to determine the critical seismic gap between two adjacent buildings with a different number of stories. The schematic diagram of the ANN model and the detailed flowchart of its algorithm are shown in Figure 1.
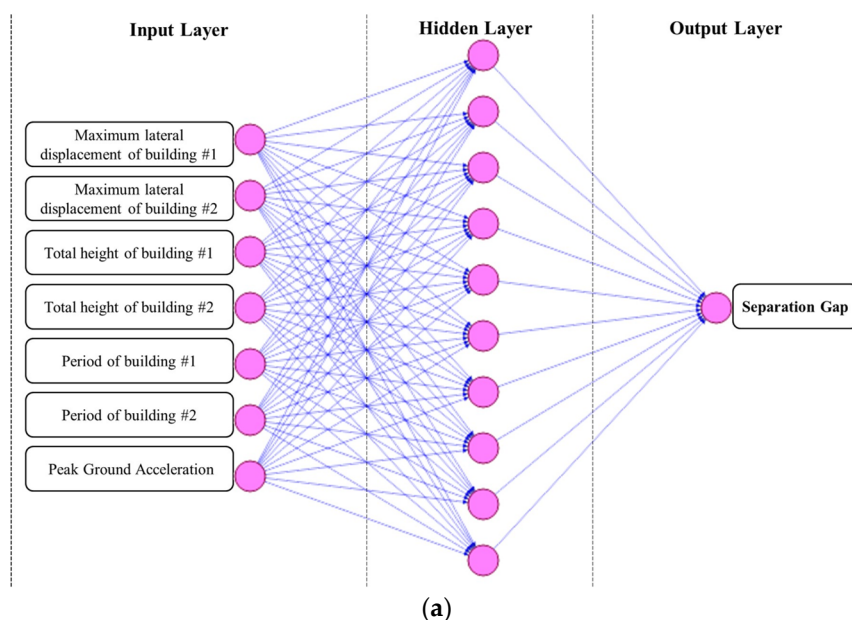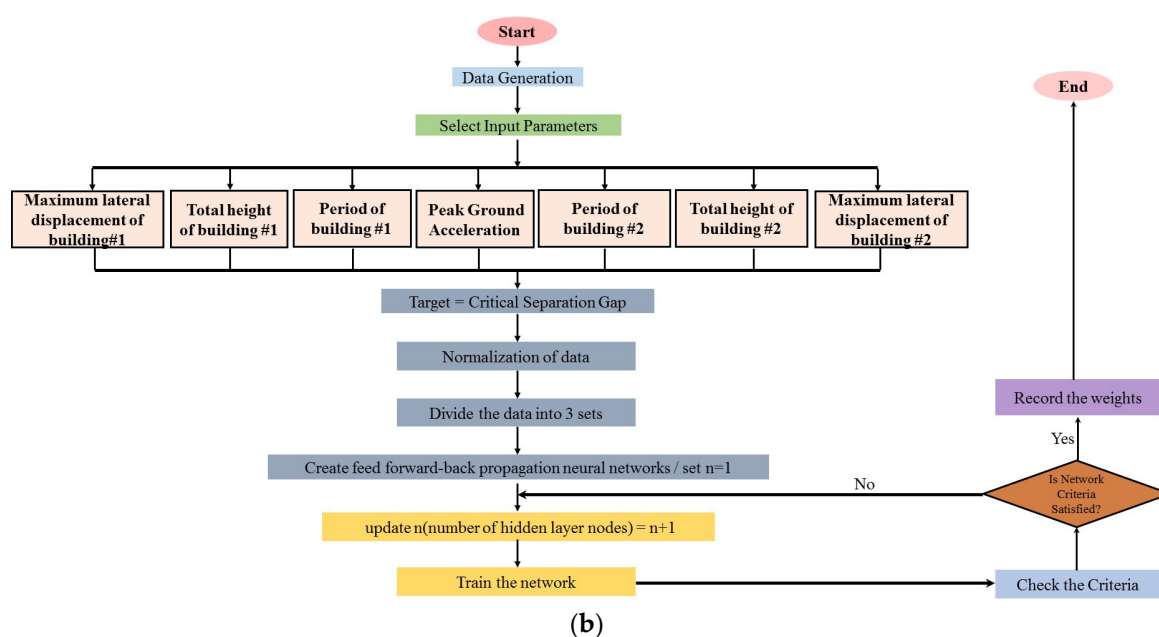

(a)

Figure 1. *Cont.*

Figure 1. (**a**) Schematic architecture of the artificial neural network (ANN) model, (**b**) flowchart of the ANN algorithm.

The details concerning the ANN analysis for a specified set of inputs can be found in a number of other publications (see [41–47], for example). Nevertheless, in order to describe the methodology of the method, an input layer is generally made by the ANN, and all of them are coordinated to find an iterative procedure between each other and automatically are analyzed in the second layer. The cell body of a neuron is connected to the dendrite of a neighboring neuron. These individual biological neurons are interconnected with the other neurons through hair-like dendrites. A group of these neurons can consist of layers of neurons, and a collection of layers can form nerve systems in the human body. Signal communications between neurons are continuously generated and delivered from one neuron to the others by firing an electrical signal generated through a chemical reaction. The other neurons receive the signal through the interfaces with the neighboring neurons, referred to as a synapse. This system is capable of learning, recalling, and generating an output corresponding to the external signals. If a system of neurons has a consistent and frequent external signal, its output signal will be consistent and thus stored in the system. On the other hand, if it is subjected to an insistent or rare signal, the memory for this type of information may vanish after receiving other signals or patterns. This biological neuron system can work collectively to handle more complicated learning to illustrate how the mathematical operations are used to mimic the major biological functionalities. Similar to biological neurons, a computational neuron has an input, a neuron cell, and an output. Each neuron is commonly connected with net-like internal weights in which complex knowledge is embedded.

The ANN types can be distinguished by the overall structure, neuron type, training data space, and learning rules, among others. Each input is weighted with an appropriate weight. The sum of the weighted inputs and the bias forms the input to the transfer function. Neurons can use any differentiable transfer function to generate their output. Backpropagation is the generalization of the Widrow–Hoff learning rule to multiple layer networks and nonlinear differentiable transfer functions. Since networks with biases, a sigmoid layer, and a linear output layer are capable of approximating any function with a finite number of discontinuities, input vectors and the corresponding target vectors are used to train a network until it can approximate a function. Standard backpropagation is a gradient descent algorithm in which the network weights are moved along the negative of the gradient of the performance function. The term backpropagation refers to the manner in which the gradient is computed for nonlinear multilayer networks. There are a number of variations on the basic algorithm

that are based on other standard optimization techniques, such as the conjugate gradient and Newton methods. Properly trained backpropagation networks tend to give reasonable answers when presented with inputs that they have never seen. Typically, a new input leads to an output similar to the correct output for the input vectors used in training that are similar to the new input being presented. This generalization property makes it possible to train a network on a representative set of input/target pairs and get good results without training the network on all possible input/output pairs.

The most common backpropagation training algorithm is Levenberg–Marquardt, which has been used in this investigation. One hidden layer has been used in the ANN modeling with sigmoid transfer functions. Before training the selected data, normalization/scaling for the whole data has been conducted. This has been done since the sigmoid transfer function has been used in the network which recognizes values between 0 and 1. In order to scale the data from 0.1 to 0.9, minimum and maximum values have been taken to use linear relationship between those values. In the ANN modeling, 60% of the whole data has been specified as the training data in which the network could be adjusted according to its error. Similarly, 20% of the database has been considered as the validating data which have been used to measure network generalization and to halt training when generalization stops improving. Finally, the remaining 20% of the whole data has been specified as the testing data which have no effect on training, providing an independent measure of the network performance during and after training.

The mean square error (MSE), which is the average squared difference between the outputs and targets, has been taken as the criterion for stopping the training of the networks. Lower values mean a better performance of the network (zero means no error). Regression values (R-values) measure the correlation between the outputs and targets in the networks: an R-value of 1 means a close relationship and in contrast, 0 means a random relationship. These two criteria (MSE and R-values) have been considered as the basis for selecting the idealized network.

The natural periods of structures, peak ground acceleration (PGA) of earthquake records, height of buildings, and peak lateral displacements of independently vibrating structures have been defined as inputs in the analysis. These chosen variables (as the representatives of the structural properties and the characteristics of earthquake records) have been considered as the input signals for the neural network and it has been tried to generate some data by repeating the analysis for some ground motions and also buildings with different heights and periods in order to form a generalized database by which the target (critical separation gap) could be predicted. For instance, the maximum lateral displacement is the maximum displacement obtained from a time history analysis under a certain earthquake record. In each analysis, the required separation gap has been computed using a trial-and-error procedure.

The analysis has been focused on adjacent reinforced concrete regular buildings with a square plan of 20×20 m (see [36] to see how irregularity changes the displacement response). The height, mass, and stiffness of each story for them are equal to $h = 3$ m, $m = 30{,}000$ kg, and $k = 2 \times 10^6$ kg/m, respectively. Lumped mass models of structures, with the mass of each story lumped at the floor level, have been considered. Six models with a different number of stories (from one to six) have been analyzed. Their elastic (un-cracked) natural vibration periods, which depend directly on structural stiffness and mass, have been calculated as equal to T = 0.544 s, 1.24 s, 1.73 s, 2.215 s, 2.93 s, and 3.38 s for single-story, two-story, three-story, four-story, five-story, and six-story buildings, respectively. Two structures have been considered to be located close to one another, taking into account all possible combinations from the point of view of the different number of stories. The example of the arrangement, denoted as 3-2, indicating a three-story building adjacent to a two-story structure is presented in Figure 2.
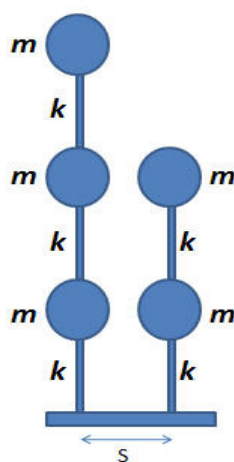
Figure 2. Model of three-story building located close to a two-story structure (arrangement 3-2).

It should be underlined that this study uses linear elastic numerical models. Previous studies have shown that inelastic behavior can significantly increase the lateral displacement responses of low-rise (short-period) buildings; whereas, for tall (long-period) buildings, inelastic behavior can reduce the lateral displacement responses to some extent (see [48–51] for example). Therefore, the results of the present study are valid for the case of buildings responding elastically. Moreover, in this study, soil–structure interaction effects are neglected assuming that the soil underneath the foundations is infinitely rigid. The inherent damping of the building is modeled using 5% Rayleigh damping. This assumption provides reasonable results when the building responds elastically. For the case of inelastic buildings, modified versions of Rayleigh damping have been proposed in the literature (see [52–55]).

Six different earthquake records have been used in the analyses, i.e., the Tabas, Imperial Valley, Loma Prieta, Landers, Kobe, and Kocaeli earthquakes (see Table 1 for details). The peak lateral displacements of independently vibrating buildings under each seismic excitation have been firstly determined. The analysis has been conducted using a Matlab-based software. The results of the time history dynamic analysis are summarized in Table 2. The graphical representation of the results is also shown in Figure 3.

Table 1. The properties of earthquake records used in the analysis.

Earthquake	Date	Magnitude	Station	PGA (cm/s^2)
Tabas	1978	7.4	Tabas	821
Imperial Valley	1979	6.5	Calexico	284
Loma Prieta	1989	6.9	Presidio	360
Landers	1992	7.3	Baker	765
Kobe	1995	7.2	JMA	338
Kocaeli	1999	7.6	Sakarya	369

Table 2. Peak lateral displacements of buildings under different earthquake records (cm).

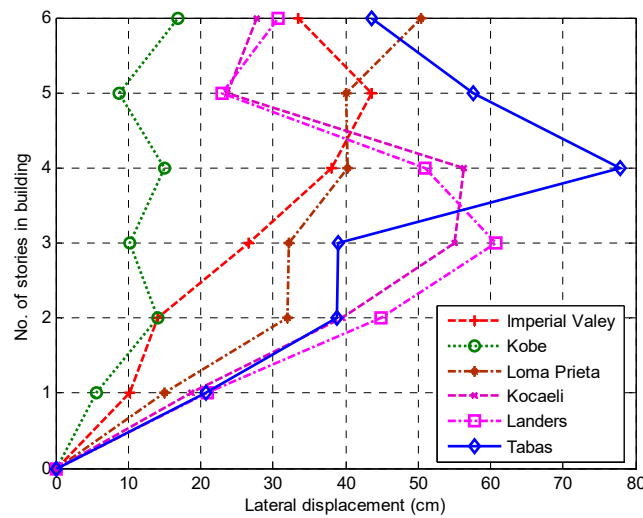| Building	Imperial Valley	Kobe	Loma Prieta	Kocaeli	Landers	Tabas
Single-story	10.25	5.66	15.1	18.63	20.86	20.67
Two-story	14.15	14.11	31.9	39.58	44.83	38.72
Three-story	26.62	10.32	32.1	55.1	60.65	38.95
Four-story	38.06	15	40.24	56.4	50.94	77.81
Five-story	43.57	8.8	40	23.73	22.87	57.52
Six-story	33.52	16.85	50.5	27.67	30.74	43.51

Figure 3. Peak lateral displacements of buildings under different earthquake records.

3. Results

Using the ANN, with the schematic diagram of the model and the detailed flowchart of its algorithm shown in Figure 1, the required seismic gap preventing pounding between adjacent structures has been determined for different structural arrangements and earthquake records. The results of the analysis are summarized in Table 3. Moreover, the graphical relation between the required seismic gap and the PGA of ground motions considered in the ANN analysis for different structural arrangements are also presented in Figure 4.

Table 3. Required seismic gap obtained from the analysis using ANN (cm).

Arrangement	Imperial Valley	Kobe	Loma Prieta	Kocaeli	Landers	Tabas
1-1	0	0	0	0	0	0
1-2	15.5	12	28	25	25	40
1-3	20.2	10.5	33	25	30	35
1-4	24.1	8	32	35	30	40
1-5	18	8	22	23	30	40
1-6	17	8	25	25	25	30
2-1	15.5	12	28	25	25	40
2-2	0	0	0	0	0	0
2-3	25	22	50	70	70	63
2-4	40	19	52	72	72	65
2-5	29	15	48	58	53	67
2-6	30	18	45	50	56	55
3-1	20.2	10.5	33	25	30	35
3-2	25	22	50	70	70	63
3-3	0	0	0	0	0	0
3-4	55	15	60	90	85	90
3-5	50	13	60	63	70	80
3-6	48	14	47	70	60	60
4-1	24.1	8	32	35	30	40
4-2	40	19	52	72	72	65
4-3	55	15	60	90	85	90
4-4	0	0	0	0	0	0
4-5	65	17	65	65	75	80
4-6	55	25	73	74	65	65
5-1	18	8	22	23	30	40

Table 3. *Cont.*

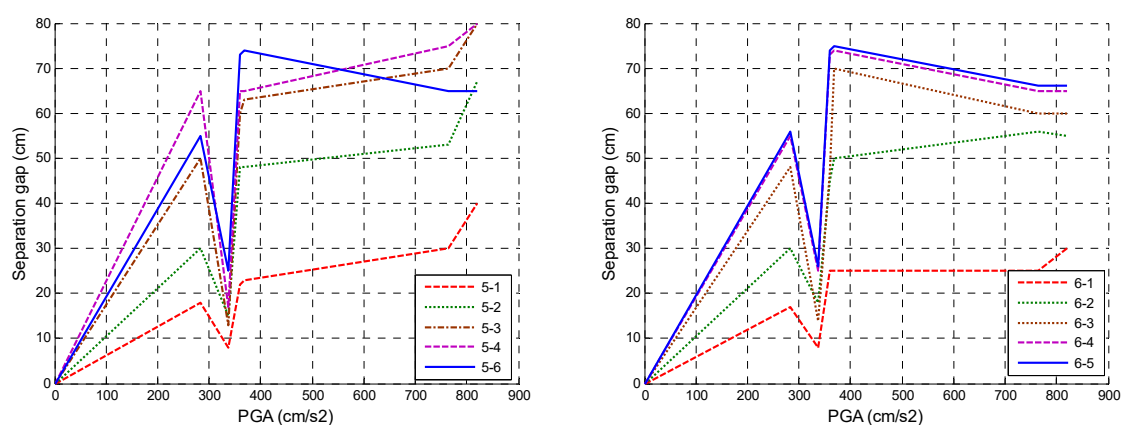| Arrangement	Imperial Valley	Kobe	Loma Prieta	Kocaeli	Landers	Tabas
5-2	29	15	48	58	53	67
5-3	50	13	60	63	70	80
5-4	65	17	65	65	75	80
5-5	0	0	0	0	0	0
5-6	56	26	74	74	67	69
6-1	17	8	25	25	25	30
6-2	30	18	45	50	56	55
6-3	48	14	47	70	60	60
6-4	55	25	73	74	65	65
6-5	56	26	74	74	67	69
6-6	0	0	0	0	0	0
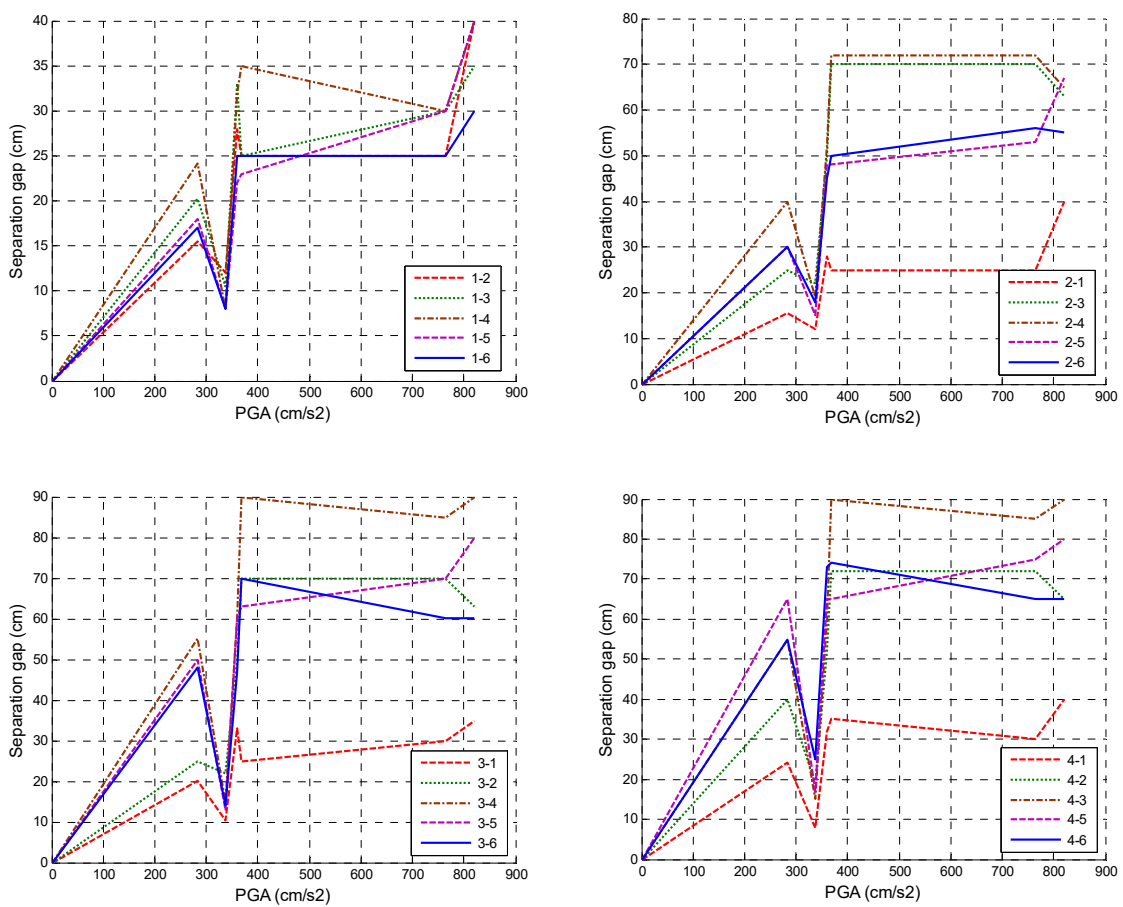
Figure 4. *Cont.*

Figure 4. Required seismic gap with relation to the peak ground acceleration (PGA) of earthquake records for different structural arrangements.

It can be seen from Table 3 that zero seismic gaps have been obtained for the cases when two identical buildings (arrangements: 1-1, 2-2, 3-3, 4-4, 5-5, 6-6) have been considered under different earthquakes. This situation results from the fact that the ground motions acting on both structures have been considered to be uniform and the in-phase structural vibrations take place in such a case. It should be underlined, however, that the out-of-phase vibrations of identical structures (with exactly the same heights and natural periods) might occur in reality if the spatial seismic effects related to the propagation of the seismic wave play an important role [56,57]. These effects, which result in non-uniform earthquake excitation, include the following: difference in the arrival times of seismic wave at various locations (wave passage effect), loss of coherency of seismic wave due to scattering in the heterogeneous medium of the ground as well as due to differential superimposition of waves arriving from an extended source (incoherence effect), and spatially varying local soil conditions (site response effect) [58].
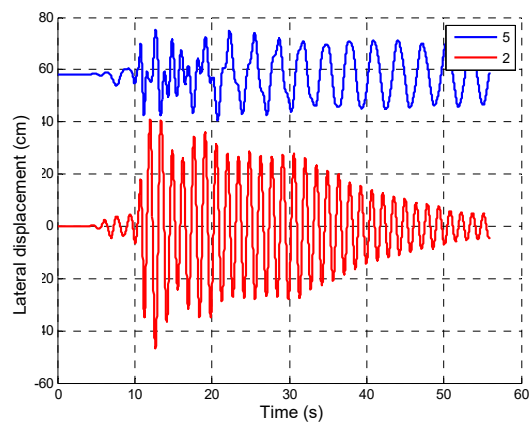
4. Verification

The results concerning the required seismic gap preventing pounding between adjacent structures (Table 3 and Figure 4) have been extensively verified for different structural arrangements and earthquake records. In this section, a representative example of the verification analysis is presented. It concerns a two-story building ($h_i = 6$ m, $T_i = 1.24$ s) located close to a five-story structure ($h_j = 15$ m, $T_j = 2.93$ s) which are exposed to the Imperial Valley (PGA = 284 cm/s^2), Kocaeli (PGA = 369 cm/s^2), and Tabas (PGA = 821 cm/s^2) earthquakes. The peak lateral displacements of independently vibrating buildings are equal to 14.15, 39.58, and 38.72 cm for the two-story structure, and 43.57, 23.73, and 57.52 cm for the five-story building under the Imperial Valley, Kocaeli, and Tabas earthquake records, respectively (see Table 2). The required seismic gap preventing pounding between adjacent structures obtained from the ANN analysis is equal to 29, 58, and 67 cm, respectively (see Table 3). The response time histories for both buildings are shown in Figure 5 for all three seismic excitations. It should be explained in this place that the initial distance, equal to the calculated seismic gap (i.e., 29, 58, 67 cm), has been introduced between two time histories of both structures in the figure in order to trace their relative displacement easily and check whether they collide during the time of the earthquake. It can be seen from Figure 5 that the calculated seismic gap is really large enough to prevent structural collisions, and it is just appropriate for the three cases of ground motions. The same conclusion has been obtained for all other structural arrangements and seismic excitations. In some cases, the seismic gap has been calculated to be so small that adjacent buildings are able nearly to touch each other during the time of the earthquake, and also zero gap sizes have been determined for identical structures. It has to be underlined, however, that the possible overlapping between the time histories of the two adjacent
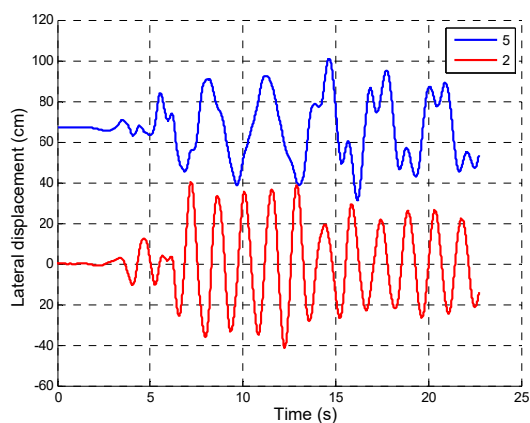
buildings has never been observed, indicating that pounding has not taken place. The above confirms the accuracy of the methodology based on the ANN which has been applied in the verification analysis.
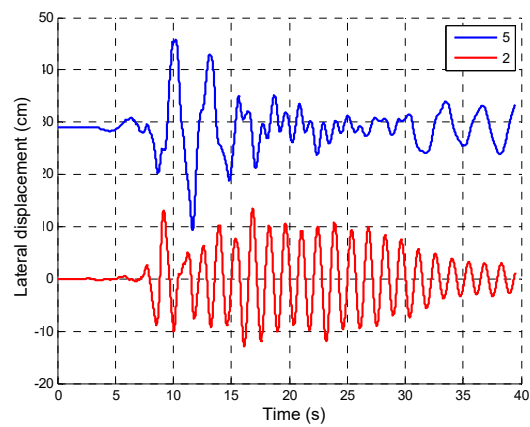
(**a**)

(**b**)

(**c**)

Figure 5. Examples of the results of the verification analysis for a two-story building located close to a five-story structure (arrangement 2-5) under three earthquake records: (**a**) Imperial Valley earthquake, seismic gap: 29 cm, (**b**) Kocaeli earthquake, seismic gap: 58 cm, (**c**) Tabas earthquake, seismic gap: 67 cm.

5. Validation

In order to validate the method for other structural parameters, the study has been further extended for buildings with different values of height, mass, and stiffness of each story for both buildings. This section presents a representative example of the validation analysis conducted for the following values: h = 3 m, m = 34,350 kg and k = 1.2·10^6 kg/m. It concerns a single-story, two-story, four-story, and five-story building located close to a three-story structure which is exposed to the Loma Prieta earthquake record (PGA = 360 cm/s^2). The natural vibration period for the single-story, two-story, four-story, and five-story structures is equal to 0.75, 1.72, 3.06, and 3.55 s, while the peak lateral displacement of the independently vibrating left building is equal to 23.34, 28.16, 43.18, and 45.36 cm, respectively. On the other hand, the natural vibration period and the peak lateral displacement of the independently vibrating three-story right building is equal to 2.38 s and 26.08 cm, respectively. The required seismic gap preventing pounding between adjacent structures has been calculated from the ANN analysis as equal to 33.9, 33.0, 52.6, 56.26 cm, for the arrangement 1-3, 2-3, 4-3, and 5-3, respectively. The examples of the response time histories for both buildings separated by such gap sizes are shown in Figure 6. It can be seen from the figure that the calculated seismic gap is really large enough to prevent structural collisions, and it is just appropriate for the Loma Prieta earthquake. The same conclusion has been obtained for all other structural arrangements, seismic excitations, and structural parameters. In some cases, the seismic gap has been calculated to be so small that adjacent buildings are able nearly to touch each other during the time of the earthquake. It has to be underlined, however, that the possible overlapping between the time histories of the two adjacent buildings has never been observed, indicating that pounding has not taken place. The above confirms the accuracy of the methodology based on the ANN which has been applied in the validation analysis for different cases and conditions.
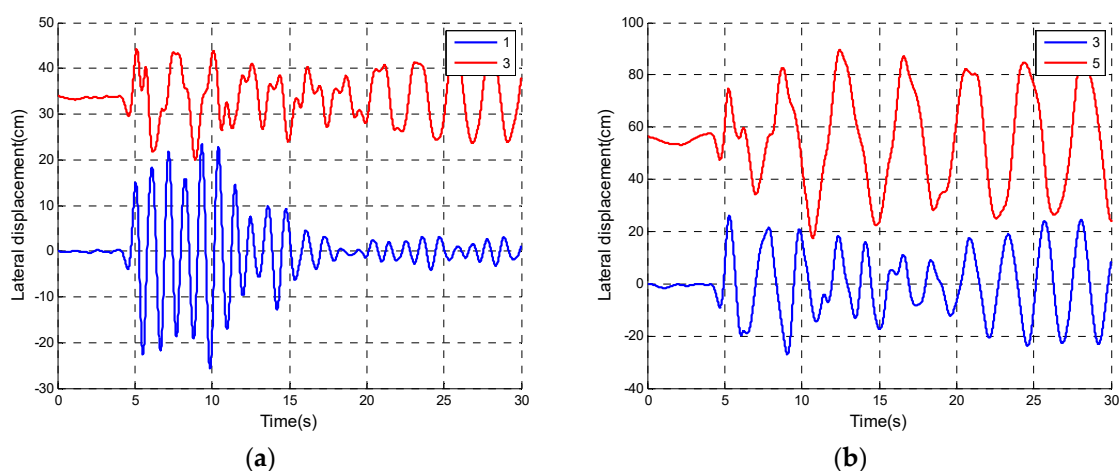

Figure 6. Examples of the results of the validation analysis under the Loma Prieta earthquake record: (**a**) arrangement 1-3, seismic gap: 33.9 cm, (**b**) arrangement 5-3, seismic gap: 56.26 cm.

6. Parametric Analysis

In the final stage of the investigation, a parametric analysis has been conducted for various earthquakes scaled to different values of the PGA. This section presents a representative example of the analysis conducted for the following values: h = 3 m, m = 34,350 kg, and k = 1.2 · 10^6 kg/m (compare previous section). It concerns a single-story building located close to a two-story, three-story, four-story, and five-story structure. Using the ANN, the required seismic gap preventing pounding between adjacent structures has been determined for different structural arrangements and seismic excitations scaled to different values of the PGA. The results of the parametric analysis are shown in Figure 7 (vertical lines in the figure refer to the original PGA levels of specific earthquakes). It can be seen from the figure that the increase in the PGA of earthquake records leads to a substantial, nearly

uniform, increase in the required seismic gap between structures, which mainly results from larger lateral structural displacements. Figure 7 indicates that the smallest values of the seismic gap have been obtained for arrangement 1-5 under the Kobe earthquake record. On the other hand, the largest in-between gap sizes have been determined for arrangement 1-2 for the Tabas seismic excitation.
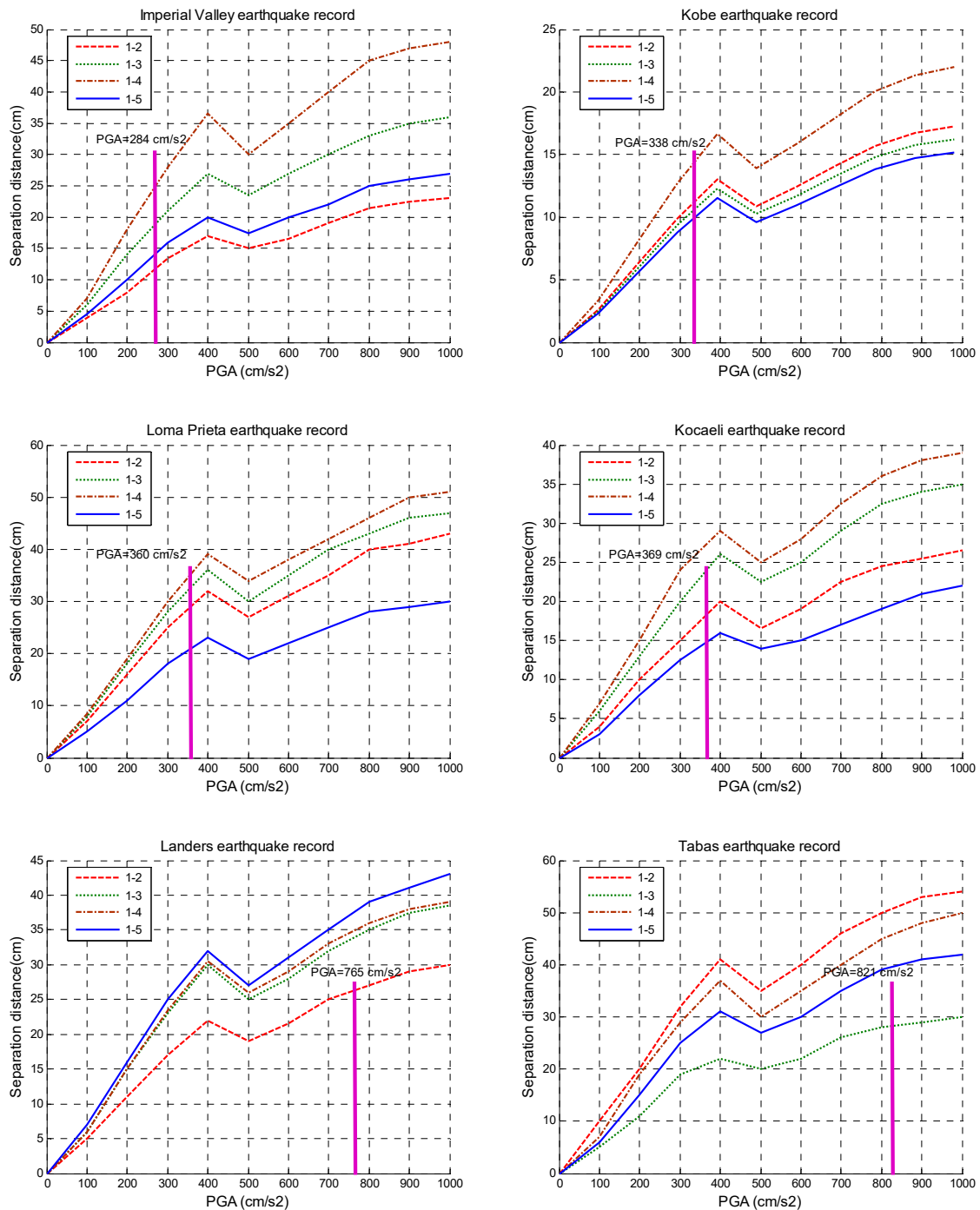

Figure 7. Examples of the results of the parametric analysis under various earthquakes scaled to different PGA values.

7. Concluding Remarks

The results of the investigation focused on using the ANN method to conduct the evaluation of the optimum gap size between adjacent buildings so as to prevent their collisions during seismic

excitations have been shown in the paper. In the study, two adjacent structures have been subjected to different earthquake records. Six lumped mass models of buildings with a different number of stories (from one to six) have been considered. The earthquake characteristics and the parameters of buildings have been defined as inputs in the ANN analysis.

Using the ANN, the required seismic gap preventing pounding between adjacent structures has been firstly determined for specified structural arrangements and earthquake records. The obtained values have been extensively verified. The results of the verification analysis show that the seismic gaps are large enough to prevent structural collisions, and they are just appropriate for all considered structural arrangements and seismic excitations which confirms the accuracy of the method applied.

In order to validate the method for other structural parameters, the study has been further extended for buildings with different values of height, mass, and stiffness of each story for both buildings. The results of the validation analysis indicate that the calculated seismic gaps using the ANN method are large enough to prevent structural collisions, and they are just appropriate for all other structural arrangements, seismic excitations, and structural parameters which validates the accuracy of the method applied for different cases and conditions.

Finally, the parametric analysis has been conducted for various earthquakes scaled to different values of the PGA. The results of this analysis show that the increase in the PGA of earthquake records leads to a substantial, nearly uniform, increase in the required separation gap between structures, which mainly results from larger lateral structural displacements.

The above conclusions clearly indicate that the ANN method can be successfully used to determine the minimal distance between two adjacent buildings preventing their collisions during different seismic excitations.

Author Contributions: Conceptualization, S.M.K., H.N. and S.M.N.R.; methodology, S.M.K., H.N., S.M.N.R., R.C.B., B.S. and R.J.; software, S.M.K. and S.M.N.R.; validation, S.M.K., H.N., S.M.N.R., R.C.B., B.S. and R.J.; formal analysis, S.M.K. and S.M.N.R.; investigation, S.M.K. and S.M.N.R.; writing—original draft preparation, S.M.K, H.N., S.M.N.R. and R.C.B.; writing—review and editing, B.S. and R.J. All authors have read and agreed to the published version of the manuscript.

References

1. Anagnostopoulos, S.A. Pounding of building in series during earthquakes. *Earthq. Eng. Struct. Dyn.* **1988**, *16*, 443–456. [CrossRef]

2. Miari, M.; Choong, K.K.; Jankowski, R. Seismic pounding between adjacent buildings: Identification of parameters, soil interaction issues and mitigation measures. *Soil Dyn. Earthq. Eng.* **2019**, *121*, 135–150. [CrossRef]

3. Jankowski, R. Pounding between superstructure segments in multi-supported elevated bridge with three-span continuous deck under 3D non-uniform earthquake excitation. *J. Earthq. Tsunami* **2015**, *9*, 1550012. [CrossRef]

4. Rahman, A.M.; Carr, A.J.; Moss, P.J. Structural pounding of adjacent multi-storey structures considering soil flexibility effects. In Proceedings of the 12th World Conference on Earthquake Engineering, Auckland, New Zealand, 30 January–4 February 2000.

5. Favvata, M.J. Minimum required separation gap for adjacent RC frames with potential inter-story seismic pounding. *Eng. Struct.* **2017**, *152*, 643–659. [CrossRef]

6. Khatami, S.M.; Naderpour, H.; Barros, R.C.; Jakubczyk-Gałczyńska, A.; Jankowski, R. Effective formula for impact damping ratio for simulation of earthquake-induced structural pounding. *Geosciences* **2019**, *9*, 347. [CrossRef]

7. Favvata, M.J.; Karayannis, C.G.; Liolios, A.A. Influence of exterior joint effect on the inter-story pounding interaction of structures. *J. Struct. Eng. Mech.* **2009**, *33*, 113–136. [CrossRef]

8. Sołtysik, B.; Jankowski, R. Non-linear strain rate analysis of earthquake-induced pounding between steel buildings. *Int. J. Earth Sci. Eng.* **2013**, *6*, 429–433.

9. Elwardany, H.; Seleemah, A.; Jankowski, R. Seismic pounding behavior of multi-story buildings in series considering the effect of infill panels. *Eng. Struct.* **2017**, *144*, 139–150. [CrossRef]

10. Abdel Raheem, S.E.; Fooly, M.Y.M.; Abdel Shafy, A.G.A.; Abbas, Y.A.; Omar, M.; Abdel Latif, M.M.S.; Mahmoud, S. Seismic pounding effects on adjacent buildings in series with different alignment configurations. *Steel Compos. Struct.* **2018**, *28*, 289–308.

11. Elwardany, H.; Seleemah, A.; Jankowski, R.; El-Khoriby, S. Influence of soil-structure interaction on seismic pounding between steel frame buildings considering the effect of infill panels. *Bull. Earthq. Eng.* **2019**, *17*, 6165–6202. [CrossRef]

12. Khatami, S.M.; Naderpour, H.; Barros, R.C.; Jakubczyk-Gałczyńska, A.; Jankowski, R. Determination of peak impact force for buildings exposed to structural pounding during earthquakes. *Geosciences* **2020**, *10*, 18. [CrossRef]

13. Rosenblueth, E.; Meli, R. The 1985 earthquake: Causes and effects in Mexico City. *Concr. Int.* **1986**, *8*, 23–34.

14. Anagnostopoulos, S.A. Earthquake induced pounding: State of the art. In Proceedings of the 10th European Conference on Earthquake Engineering, Vienna, Austria, 28 August–2 September 1994; pp. 897–905.

15. Kasai, K.; Maison, B.F. Building pounding damage during the 1989 Loma Prieta earthquake. *Eng. Struct.* **1997**, *19*, 195–207. [CrossRef]

16. International Code Council Inc. *IBC: International Building Code*; International Code Council Inc.: Country Club Hills, IL, USA, 2009.

17. European Committee for Standardization. *Eurocode 8: Design of Structures for Earthquake Resistance*; European Committee for Standardization: Brussels, Belgium, 2003.

18. Building & Housing Research Center. *Iranian Code of Practice for Seismic Resistant Design of Buildings (Standard 2800—4th Edition)*; Permanent Committee of Revising the Code of Practice for Seismic Resistant Design of Buildings, BHR: Tehran, Iran, 2017; p. 94.

19. Jeng, V.; Kasai, K.; Maison, B.F. A spectral difference method to estimate building separations to avoid pounding. *Earthq. Spectra* **1992**, *8*, 201–223. [CrossRef]

20. Filiatrault, A.; Wagner, P.; Cherry, S. Analytical prediction of experimental building pounding. *Earthq. Eng. Struct. Dyn.* **1995**, *24*, 1131–1154. [CrossRef]

21. Naderpour, H.; Barros, R.C.; Khatami, S.M. Prediction of critical distance between two MDOF systems subjected to seismic excitation in terms of artificial neural networks. *Period. Polytech. Civ. Eng.* **2017**, *61*, 516–529. [CrossRef]

22. Der Kiureghian, A. A response spectrum method for random vibration analysis of MDF systems. *Earthq. Eng. Struct. Dyn.* **1981**, *9*, 419–435. [CrossRef]

23. Penzien, J. Evaluation of building separation gap required to prevent pounding during strong earthquakes. *Earthq. Eng. Struct. Dyn.* **1997**, *26*, 849–858. [CrossRef]

24. Garcia, D.L. Separation between adjacent non-linear structures for prevention of seismic pounding. In Proceedings of the 13th World Conference on Earthquake Engineering, Vancouver, BC, Canada, 1–6 August 2004.

25. Kasai, K.; Jagiasi, A.R.; Jeng, V. Inelastic vibration phase theory for seismic pounding mitigation. *J. Struct. Eng.* **1996**, *122*, 1136–1146. [CrossRef]

26. Lopez-Garcia, D.; Soong, T.T. Evaluation of current criteria in predicting the separation necessary to prevent seismic pounding between nonlinear hysteretic structural systems. *Eng. Struct.* **2009**, *31*, 1217–1229. [CrossRef]

27. Zhang, W.S.; Xu, Y.L. Dynamic characteristics and seismic response of adjacent buildings linked by discrete dampers. *Earthq. Eng. Struct. Dyn.* **1999**, *28*, 1163–1185. [CrossRef]

28. Matsagar, V.A.; Jangid, R.S. Viscoelastic damper connected to adjacent structures involving seismic isolation. *J. Civ. Eng. Manag.* **2005**, *11*, 309–322. [CrossRef]

29. Polycarpou, P.C.; Komodromos, P. Numerical investigation of potential mitigation measures for pounding of seismically isolated building. *Earthq. Struct.* **2011**, *2*, 1–24. [CrossRef]

30. Raheem, S.E.A. Mitigation measures for earthquake induced pounding effects on seismic performance of adjacent buildings. *Bull. Earthq. Eng.* **2014**, *12*, 1705–1724. [CrossRef]

31. Khatami, S.M.; Naderpour, H.; Razavi, S.M.N.; Barros, R.C.; Jakubczyk-Gałczyńska, A.; Jankowski, R. Study on methods to control interstory deflections. *Geosciences* **2020**, *10*, 75. [CrossRef]

32. Anajafi, H.; Ghomi-Gharaei, A.; Ghorbani-Tanha, A.K. The effect of soil-structure-foundation interaction on lateral structural displacement and comparison with design code requirements. In Proceedings of the SE-50EEE International Conference on Earthquake Engineering, Skopje, Macedonia, 29–31 May 2013.

33. Jeng, V.; Tzeng, W.L. Assessment of seismic pounding hazard for Taipei City. *Eng. Struct.* **2000**, *22*, 459–471. [CrossRef]

34. Bazan, E.; Bielak, J. Earthquake response of nonlinear building-foundation systems. *Dev. Geotech. Eng.* **1987**, *43*, 13–24.

35. Ghomi-Gharaei, A.; Anajafi, H.; Ghorbani-Tanha, A.K. Comparison of footing design codes criteria and foundation effects on structural seismic behavior. In Proceedings of the 4th International Conference on Concrete and Development, Tehran, Iran, 29 April–1 May 2013.

36. Anajafi, H.; Medina, R.A. Lessons learned from evaluating the responses of instrumented buildings in the United States: The effects of supporting building characteristics on floor response spectra. *Earthq. Spectra* **2019**, *35*, 159–191. [CrossRef]

37. Goetz, T. *The Decision Tree: How to Make Better Choices and Take Control of Your Health*; Rodale Books: Emmaus, PA, USA, 2010.

38. Schmidt, V. *Stochastic Geometry, Spatial Statistics and Random Fields: Models and Algorithms*; Springer: Berlin/Heidelberg, Germany, 2015.

39. Jankowski, R.; Walukiewicz, H. Modeling of two-dimensional random fields. *Probabilistic Eng. Mech.* **1997**, *12*, 115–121. [CrossRef]

40. Siemaszko, A.; Jakubczyk-Gałczyńska, A.; Jankowski, R. The idea of using Bayesian networks in forecasting impact of traffic-induced vibrations transmitted through the ground on residential buildings. *Geosciences* **2019**, *9*, 339. [CrossRef]

41. Rojas, R. *Neural Networks: A Systematic Introduction*; Springer Science & Business Media: Berlin/Heidelberg, Germany, 2013.

42. Hüsken, M.; Jin, Y.; Sendhoff, B. Structure optimization of neural networks for evolutionary design optimization. *Soft Comput.* **2005**, *9*, 21–28. [CrossRef]

43. Naderpour, H.; Kheyroddin, A.; Amiri, G.G. Prediction of FRP-confined compressive strength of concrete using artificial neural networks. *Compos. Struct.* **2010**, *92*, 2817–2829. [CrossRef]

44. Naderpour, H.; Rafiean, A.H.; Fakharian, P. Compressive strength prediction of environmentally friendly concrete using artificial neural networks. *J. Build. Eng.* **2018**, *16*, 213–219. [CrossRef]

45. Ahmadi, M.; Naderpour, H.; Kheyroddin, A. Utilization of artificial neural networks to prediction of the capacity of CCFT short columns subject to short term axial load. *Arch. Civ. Mech. Eng.* **2014**, *14*, 510–517. [CrossRef]

46. Naderpour, H.; Nagai, K.; Fakharian, P.; Haji, M. Innovative models for prediction of compressive strength of FRP-confined circular reinforced concrete columns using soft computing methods. *Compos. Struct.* **2019**, *215*, 69–84. [CrossRef]

47. Kamgar, R.; Naderpour, H.; Komeleh, H.E.; Jakubczyk-Gałczyńska, A.; Jankowski, R. A proposed soft computing model for ultimate strength estimation of FRP-confined concrete cylinders. *Appl. Sci.* **2020**, *10*, 1769. [CrossRef]

48. Chenouda, M.; Ayoub, A. Inelastic displacement ratios of degrading systems. *J. Struct. Eng.* **2008**, *134*, 1030–1045. [CrossRef]

49. Chopra, A.K.; Chintanapakdee, C. Inelastic deformation ratios for design and evaluation of structures: Single-degree-of-freedom bilinear systems. *J. Struct. Eng.* **2004**, *130*, 1309–1319. [CrossRef]

50. Iervolino, I.; Chioccarelli, E.; Baltzopoulos, G. Inelastic displacement ratio of near-source pulse-like ground motions. *Earthq. Eng. Struct. Dyn.* **2012**, *41*, 2351–2357. [CrossRef]

51. Anajafi, H.; Poursadr, K.; Roohi, M.; Santini-Bell, E. Effectiveness of seismic isolation for long-period structures subject to far-field and near-field excitations. *Front. Built Env.* **2020**, *6*, 24. [CrossRef]

52. Léger, P.; Dussault, S. Seismic-energy dissipation in MDOF structures. *J. Struct. Eng.* **1992**, *118*, 1251–1269. [CrossRef]

53. Anajafi, H.; Medina, R.A.; Santini-Bell, E. Effects of the improper modeling of viscous damping on the first-mode and higher-mode dominated responses of base-isolated buildings. *Earthq. Eng. Struct. Dyn.* **2020**, *49*, 51–73. [CrossRef]

54. Charney, F.A. Unintended consequences of modeling damping in structures. *J. Struct. Eng.* **2008**, *134*, 581–592. [CrossRef]

55. Chopra, A.K.; McKenna, F. Modeling viscous damping in nonlinear response history analysis of buildings for earthquake excitation. *Earthq. Eng. Struct. Dyn.* **2016**, *45*, 193–211. [CrossRef]

56. Jankowski, R. Non-linear FEM analysis of pounding-involved response of buildings under non-uniform earthquake excitation. *Eng. Struct.* **2012**, *37*, 99–105. [CrossRef]

57. Burkacki, D.; Wójcik, M.; Jankowski, R. Numerical investigation on behaviour of cylindrical steel tanks during mining tremors and moderate earthquakes. *Earthq. Struct.* **2020**, *18*, 97–111.

58. Der Kiureghian, A. A coherency model for spatially varying ground motions. *Earthq. Eng. Struct. Dyn.* **1996**, *25*, 99–111. [CrossRef]